JUSAN SCIENCE

Journal of Engineering and Environmental Systems

ISSN (Print): 3135-2510; ISSN (Online): 3135-2529

journal homepage: https://jusanscience.com/journals/jees

Research Article

Biomass-Derived Reduced Graphene Oxide from Coconut Shell Waste as a Multifunctional Adsorbent for Heavy Metal and Dye Removal from Water

Prince Howard[1], Vigil Ahormegah[1], Boansi Adu Ababio[1], Harry Kwaku Megbenu[2*]

[1]School of Physical Sciences, Department of Chemistry, University of Cape Coast, Ghana
[2]Department of Chemical and Materials Engineering, School of Engineering and Digital Science

Corresponding author email: harry.megbenu@nu.edu.kz

https://doi.org/10.66973/jees.26.006

Article info:

Received: 04 May 2026 / Revised: 05 June 2026 / Accepted: 05 June 2026 / Published: 07 June 2026

Howard, P., Ahormegah, V., Adu Ababio, B., & Kwaku Megbenu, H. (2026). Biomass-Derived Reduced Graphene Oxide from Coconut Shell Waste as a Multifunctional Adsorbent for Heavy Metal and Dye Removal from Water. *Journal of Engineering and Environmental Systems*, *1*(1), 68-79. https://doi.org/10.66973/jees.26.006

Abstract: The development of sustainable adsorbents from renewable biomass has attracted considerable attention for wastewater treatment applications. In this study, reduced graphene oxide (rGO) was successfully synthesized from coconut shell waste through carbonization, modified Hummer's oxidation, and chemical reduction. The resulting material was evaluated for the removal of Cd^{2+}, Ni^{2+}, Pb^{2+}, and methylene blue (MB) from aqueous solutions. Morphological characterization by SEM and TEM confirmed the successful transformation of the biomass precursor into graphene-like nanosheets and the formation of a more ordered graphitic structure following reduction. The effects of solution pH, contact time, adsorbent dosage, and initial pollutant concentration on adsorption performance were systematically investigated. Optimum adsorption was achieved at pH 7, an adsorbent dosage of 50 mg, and an equilibrium time of 180 min. Under optimized conditions, the maximum adsorption capacities of rGO reached 110, 102, 95, and 108 mg g^{-1} for Cd^{2+}, Ni^{2+}, Pb^{2+}, and MB, respectively. Compared with graphene oxide-like nanosheets, the reduction process improved adsorption performance by up to 50%, highlighting the beneficial role of restoring graphitic domains and enhancing surface accessibility. Furthermore, the synthesized rGO exhibited excellent regeneration performance, retaining more than 87% of its initial adsorption capacity after five consecutive adsorption–desorption cycles.

Keywords: biomass-derived reduced graphene oxide; coconut shell-derived rGO; coconut shell waste; heavy metal removal; dye removal; sustainable adsorbent; wastewater treatment.

https://doi.org/10.66973/jees.26.006

1 Introduction

Water pollution caused by the continuous discharge of toxic heavy metals and synthetic organic dyes has become one of the most serious environmental challenges associated with rapid industrialization and urban development. Industrial sectors such as electroplating, mining, battery manufacturing, leather processing, textile dyeing, and pharmaceutical production release substantial quantities of hazardous pollutants into aquatic ecosystems, leading to severe environmental and public health concerns [1], [2]. Heavy metals such as cadmium (Cd^{2+}), nickel (Ni^{2+}), and lead (Pb^{2+}) are non-biodegradable and can accumulate within biological systems through biomagnification, resulting in long-term toxicological effects including neurological disorders, kidney damage, carcinogenicity, and developmental abnormalities [3]. Similarly, synthetic dyes such as methylene blue (MB) are highly stable aromatic compounds that resist natural degradation and significantly reduce light penetration in water bodies, thereby affecting photosynthetic activity and disturbing aquatic ecological balance [4]. Due to their high persistence and toxicity, the removal of heavy metals and dye contaminants from wastewater remains a major priority in environmental remediation research.

Various physicochemical and biological treatment technologies have been developed for wastewater purification, including chemical precipitation, membrane filtration, ion exchange, coagulation–flocculation, photocatalysis, and biological degradation [5], [6]. Although these approaches have demonstrated varying degrees of effectiveness, many suffer from important limitations such as high operational cost, membrane fouling, sludge generation, incomplete pollutant removal, and poor performance at low contaminant concentrations [7]. Among the available treatment methods, adsorption has emerged as one of the most promising strategies owing to its operational simplicity, high removal efficiency, low energy requirement, and ability to treat a wide range of pollutants simultaneously [8]. The efficiency of adsorption processes is strongly dependent on the physicochemical properties of the adsorbent material, particularly its surface area, porosity, surface functional groups, and structural stability [9].

In recent years, graphene-based materials have attracted significant scientific attention as advanced adsorbents for environmental remediation applications due to their exceptional physicochemical properties [10], [11]. Graphene oxide (GO), a two-dimensional oxidized derivative of graphene, possesses abundant oxygen-containing functional groups such as hydroxyl, epoxy, carbonyl, and carboxyl groups distributed across its basal planes and edges [12]. These functionalities provide numerous active adsorption sites capable of interacting with metal ions and organic molecules through electrostatic attraction, hydrogen bonding, ion exchange, and surface complexation mechanisms [13]. Furthermore, the reduction of GO into reduced graphene oxide (rGO) partially restores the conjugated sp^2 carbon network, resulting in improved electrical conductivity, enhanced structural ordering, increased hydrophobicity, and stronger π–π interactions with aromatic contaminants [14]. Consequently, rGO has demonstrated superior adsorption performance compared to GO for the removal of both heavy metals and organic dyes from aqueous environments [15]. The synthesis route employed for graphene-based materials plays a critical role in determining their structural characteristics and adsorption performance. Among the various preparation methods, the modified Hummers oxidation approach remains one of the most widely applied techniques due to its relatively high oxidation efficiency, scalability, and ability to produce graphene oxide-like nanosheets with abundant surface functionalities [16], [17]. Conventionally, high-purity graphite is used as the starting precursor for GO synthesis; however, the dependence on commercial graphite significantly increases production cost and limits large-scale

https://doi.org/10.66973/jees.26.006

environmental applications [18]. In response to these limitations, increasing research attention has been directed toward the development of biomass-derived carbon nanomaterials using renewable agricultural residues as sustainable carbon sources [19].

Agricultural biomass waste represents attractive precursors for graphene-like carbon materials because of their high carbon content, low cost, renewability, and environmental availability. Among various biomass resources, coconut shell waste has emerged as a particularly promising precursor due to its high lignocellulosic composition, excellent carbon yield, and widespread availability in tropical and subtropical regions [20]. The valorization of coconut shell biomass into high-value carbon nanomaterials not only reduces environmental burden associated with agricultural waste disposal but also supports circular economy and sustainable resource utilization principles [21]. Previous studies have demonstrated that coconut shell-derived graphene oxide-like materials exhibit favorable structural and surface characteristics suitable for adsorption and environmental remediation applications [22]. However, many existing investigations primarily focus on either heavy metal adsorption or dye removal individually, while comprehensive studies involving multifunctional adsorption systems capable of simultaneously removing different classes of contaminants remain limited. In addition, several previously reported studies lack detailed adsorption mechanism analysis, systematic optimization of adsorption parameters, kinetic and isotherm modeling, and regeneration investigations necessary for evaluating practical applicability [23]. Furthermore, the structural evolution from biomass-derived graphene oxide-like materials rGO and its influence on adsorption behavior remain insufficiently explored. Therefore, there is a need for a more comprehensive investigation integrating sustainable synthesis, advanced characterization, adsorption optimization, and mechanistic understanding.

In this study, biomass-derived graphene oxide-like carbon nanosheets were synthesized from coconut shell waste using a modified Hummers oxidation method, followed by reduction to produce rGO. The synthesized materials were systematically characterized using FTIR, XRD, Raman spectroscopy, SEM–EDX, TEM, and BET surface area analysis to evaluate their structural, morphological, and physicochemical properties. The adsorption performance of the prepared rGO was investigated for the removal of Cd^{2+}, Ni^{2+}, Pb^{2+}, and MB from aqueous solutions under various experimental conditions. Adsorption kinetics, isotherm behavior, and regeneration performance were further evaluated to provide insight into the adsorption mechanism and practical applicability of the material. The present work demonstrates a sustainable and cost-effective approach for converting agricultural waste into high-performance multifunctional adsorbents for wastewater treatment applications.

2 Materials and Methods

2.1 Materials and Chemicals

Coconut shell waste used as the biomass precursor was collected locally and thoroughly cleaned prior to use. Concentrated sulfuric acid (H_2SO_4, 98%), potassium permanganate ($KMnO_4$, ≥99%), sodium nitrate ($NaNO_3$, ≥99%), hydrogen peroxide (H_2O_2, 30 wt%), hydrochloric acid (HCl, 37%), sodium hydroxide (NaOH, ≥98%), and ethanol (99.5%) were obtained from Sigma-Aldrich (USA) and used without further purification. Cadmium nitrate tetrahydrate [$Cd(NO_3)_2{\cdot}4H_2O$], nickel nitrate hexahydrate [$Ni(NO_3)_2{\cdot}6H_2O$], lead nitrate [$Pb(NO_3)_2$], and methylene blue (MB) dye were purchased from Merck (Germany). Deionized water was used throughout all experimental procedures.

2.2 Preparation of Coconut Shell Biomass

Raw coconut shell waste was thoroughly washed several times with deionized water to remove adhering dust, dirt, and soluble impurities. The cleaned biomass was initially air-dried under

https://doi.org/10.66973/jees.26.006

ambient conditions for 48 h, followed by oven drying at 105 °C for 24 h to eliminate residual moisture. The dried coconut shells were mechanically crushed and ground into fine particles using a laboratory grinder. The resulting powder was sieved to obtain a uniform particle size fraction below 250 μm prior to carbonization.

2.3 Carbonization of Coconut Shell Biomass

The prepared coconut shell powder was subjected to thermal carbonization in a tubular furnace under nitrogen atmosphere. Approximately 50 g of biomass powder was placed in a ceramic crucible and heated from room temperature to 600 °C at a heating rate of 10 °C min^{-1}. The carbonization process was maintained at 600 °C for 2 h under continuous nitrogen flow to minimize oxidation during thermal decomposition. After completion of carbonization, the furnace was allowed to cool naturally to room temperature under nitrogen atmosphere. The obtained carbonized product was collected, ground into fine powder, and stored in airtight containers for subsequent oxidation treatment.

2.4 Synthesis of Biomass-Derived Graphene Oxide-like Carbon Nanosheets

Biomass-derived graphene oxide-like carbon nanosheets were synthesized from the carbonized coconut shell precursor using a modified Hummers oxidation method. In a typical synthesis procedure, 2.0 g of carbonized coconut shell powder and 1.0 g of $NaNO_3$ were dispersed in 50 mL of concentrated H_2SO_4 under continuous magnetic stirring in an ice bath to maintain the reaction temperature below 10 °C. Subsequently, 6.0 g of $KMnO_4$ was gradually added to the suspension while carefully controlling the temperature to avoid excessive exothermic reactions. After complete addition of $KMnO_4$, the reaction mixture was stirred at 35 °C for 2 h to promote oxidation and exfoliation of the carbon structure. Thereafter, 100 mL of deionized water was slowly added to the mixture, resulting in a temperature increase due to the highly exothermic nature of the reaction. The suspension was further stirred at 95 °C for 30 min. Finally, 10 mL of H_2O_2 (30 wt%) was added to terminate the oxidation process and reduce residual permanganate species, resulting in a color change from dark brown to yellowish-black. The resulting oxidized suspension was repeatedly washed with 5% HCl solution and deionized water via centrifugation until neutral pH was achieved. The obtained graphene oxide-like material was dried in a vacuum oven at 60 °C for 24 h and stored for further reduction treatment.

The overall synthesis pathway of biomass-derived rGO from coconut shell waste, including carbonization, modified Hummer's oxidation, and chemical reduction, is illustrated in Figure 1.

2.5 Reduction of Graphene Oxide-like Carbon Nanosheets to rGO

The rGO was prepared through chemical reduction of the synthesized graphene oxide-like material. Briefly, 500 mg of graphene oxide-like nanosheets was dispersed in 200 mL of deionized water and sonicated for 1 h using an ultrasonic bath to obtain a homogeneous suspension. Subsequently, hydrazine hydrate ($N_2H_4 \cdot H_2O$, 80 wt%) was added as the reducing agent at a volume ratio of 1 mL hydrazine per 100 mg of graphene oxide-like material. The reaction mixture was heated at 95 °C under continuous stirring for 4 h. During the reduction process, the suspension color gradually changed from brownish yellow to black, indicating restoration of graphitic domains and reduction of oxygen-containing functional groups. After cooling to room temperature, the obtained rGO was separated by centrifugation, repeatedly washed with deionized water and ethanol to remove residual impurities, and dried under vacuum at 60 °C for 24 h.

2.6 Characterization Techniques

Surface morphology was conducted using a scanning electron microscopy (SEM) on a JEOL JSM-7600F microscope (JEOL Ltd., Japan). Transmission electron microscopy (TEM) analysis was performed using a JEOL JEM-2100 microscope operating at 200 kV to investigate

https://doi.org/10.66973/jees.26.006

nanosheet morphology and structural evolution after reduction. MB concentrations were measured using a UV–vis spectrophotometer (Shimadzu UV-1800, Japan) at a maximum absorption wavelength of 664 nm.

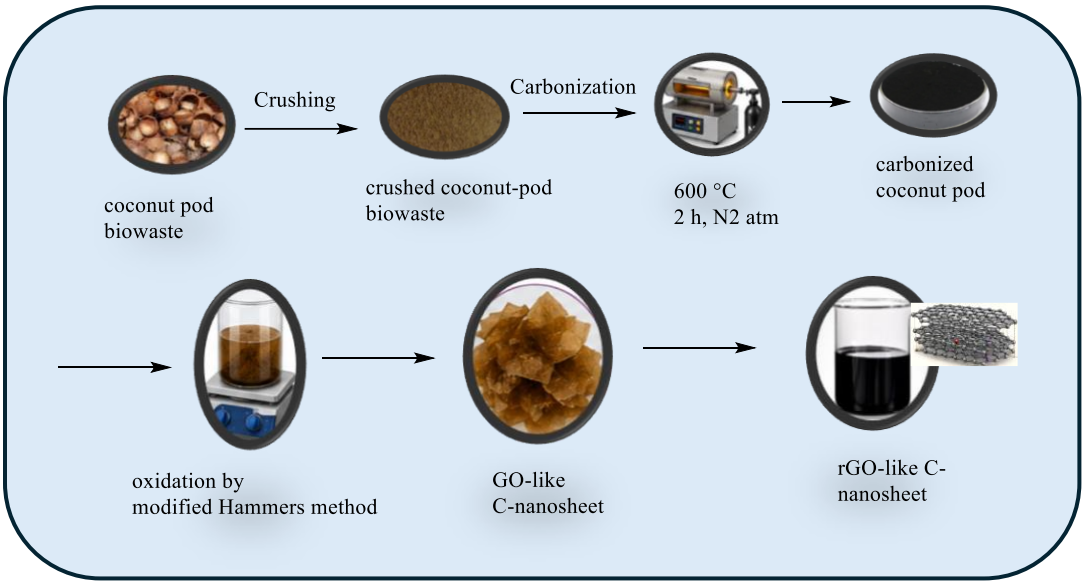

Figure 1. Synthesis pathway of biomass-derived rGO from coconut shell waste via carbonization, modified Hummer's oxidation, and chemical reduction.

2.7 Batch Adsorption Experiments

Batch adsorption experiments were performed to evaluate the adsorption performance of GO-like nanosheets and rGO toward Cd^{2+}, Ni^{2+}, Pb^{2+}, and MB from aqueous solutions. Stock solutions (1000 mg/L) of Cd^{2+}, Ni^{2+}, and Pb^{2+} were prepared from their respective nitrate salts using deionized water. Working solutions of desired concentrations were prepared through serial dilution. MB solutions were similarly prepared in deionized water. In a typical adsorption experiment, 50 mg of adsorbent was added to 100 mL pollutant solution of known concentration in a 250 mL conical flask. The suspension was agitated using a mechanical shaker at 200 rpm under controlled temperature conditions. The effects of initial pH (2–10), contact time (10–240 min), adsorbent dosage (10–100 mg), and initial pollutant concentration (10–200 mg/L) were systematically investigated. The pH of the solutions was adjusted using dilute HCl or NaOH solutions prior to adsorption. After completion of the adsorption process, the suspensions were centrifuged at 5000 rpm for 10 min, and the supernatants were analyzed for residual pollutant concentrations. All adsorption experiments were conducted in duplicate, and the average values together with standard deviations were reported.

2.8 Adsorption Capacity and Removal Efficiency Calculations

The adsorption capacity (q_e, mg/g) and removal efficiency (%) were calculated using the following equations:

$$q_e = \frac{(C_o - C_e)V}{m}$$

$$Removal\ efficiency\ (\%) = \frac{(C_o - C_e)}{C_o} \times 100$$

where C_o and C_e (mg/L) represent the initial and equilibrium pollutant concentrations, respectively, V (L) is the solution volume, and m (g) is the mass of adsorbent used.

2.9 Regeneration and Reusability Studies

The regeneration and reusability of the synthesized rGO adsorbent were evaluated through repeated

https://doi.org/10.66973/jees.26.006

adsorption–desorption cycles. After each adsorption experiment, the adsorbent was separated, washed with ethanol and deionized water, and dried at 60 °C prior to reuse. The adsorption performance after successive cycles was monitored to assess structural stability and practical applicability.

3 Results and Discussion

3.1 Morphological Characterization of GO-like Nanosheets and rGO

The morphological evolution of the synthesized materials was investigated using SEM and TEM analyses, and the results are presented in Figure 2. The SEM image of the GO-like nanosheets (Figure 2A) reveals a highly wrinkled and loosely stacked sheet-like morphology with numerous folds and cavities distributed throughout the surface. Such structural features are characteristic of oxidized graphene-based materials and indicate successful oxidation of the carbonized coconut shell precursor, leading to increased interlayer spacing and the introduction of oxygen-containing functional groups. Following chemical reduction, the morphology changed noticeably (Figure 2B). The rGO sample exhibits a more compact and densely packed layered structure with pronounced sheet aggregation. This structural rearrangement is attributed to the removal of oxygen functionalities during reduction, which promotes partial restoration of graphitic domains and stronger π–π interactions between adjacent layers. The TEM image of the GO-like material (Figure 2C) shows thin, transparent nanosheets with irregularly distributed pores, confirming the exfoliated nature of the oxidized carbon structure. In contrast, the TEM image of rGO (Figure 2D) reveals a darker and more condensed morphology, indicating increased structural ordering and restacking of graphene layers after reduction. The increased contrast observed for rGO is consistent with the reduction of oxygen-containing groups and the formation of a more graphitic carbon framework.

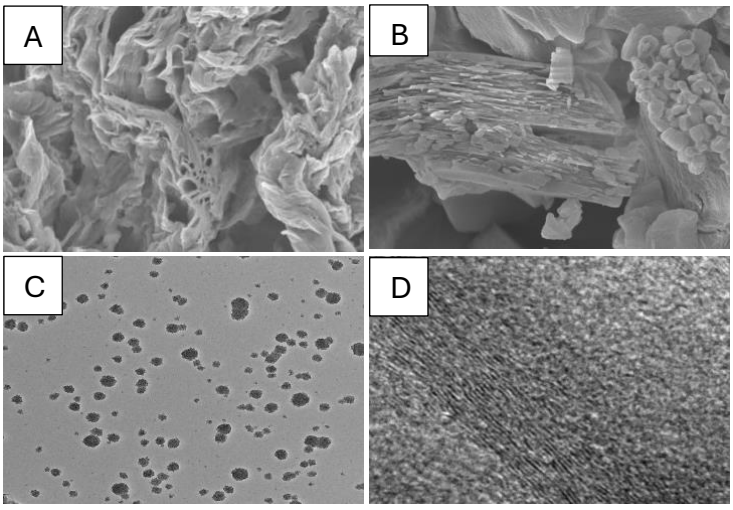

Figure 2. Morphological characterization of biomass-derived graphene oxide-like nanosheets (GO-like) and rGO: SEM images of (A) GO-like nanosheets and (B) rGO, and TEM images of (C) GO-like nanosheets and (D) rGO.

3.2 Effect of Adsorption Parameters on Pollutant Removal

The adsorption performance of biomass-derived rGO toward Cd^{2+}, Ni^{2+}, Pb^{2+}, MB was systematically evaluated by investigating the

https://doi.org/10.66973/jees.26.006

effects of solution pH, contact time, adsorbent dosage, and initial pollutant concentration. The results are presented in Figure 3 and demonstrate the strong influence of operating conditions on adsorption behaviour. As shown in Figure 3A, the adsorption capacity increased substantially with increasing solution pH from 2 to 7 for all investigated pollutants. Under strongly acidic conditions, adsorption capacities were relatively low due to the high concentration of H^+ ions competing with metal ions and dye molecules for available adsorption sites on the rGO surface. As the pH increased, deprotonation of oxygen-containing functional groups such as hydroxyl and carboxyl groups generated more negatively charged adsorption sites, thereby enhancing electrostatic attraction toward the cationic pollutants. Maximum adsorption capacities were achieved at approximately pH 7, reaching 110 mg/g for Cd^{2+}, 102 mg g^{-1} for Ni^{2+}, 95 mg/g for Pb^{2+}, and 108 mg/g for MB. A slight decrease in adsorption was observed at pH values above 7, particularly for Pb^{2+} and Ni^{2+}, which may be attributed to changes in metal speciation and the gradual saturation of adsorption sites. The results indicate that near-neutral pH conditions are most favorable for the simultaneous removal of both heavy metals and dye molecules.

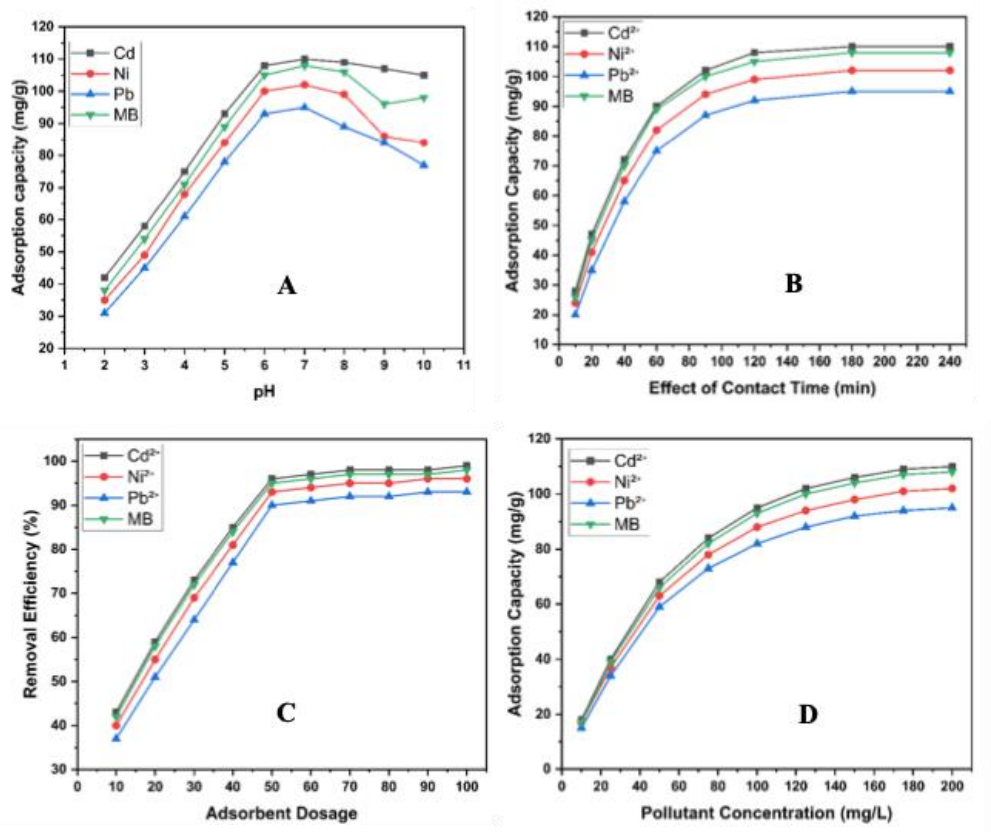

Figure 3. Effect of adsorption parameters on the removal of Cd^{2+}, Ni^{2+}, Pb^{2+}, and MB using biomass-derived rGO: (A) initial solution pH, (B) contact time, (C) adsorbent dosage, and (D) initial pollutant concentration.

The effect of contact time on adsorption capacity is presented in Figure 3B. For all pollutants, adsorption proceeded rapidly during the initial stages of the process, with a significant proportion of the total adsorption occurring within the first 60–90 min. This rapid uptake can be attributed to the abundance of readily available active sites on the external surface of the rGO nanosheets. As

https://doi.org/10.66973/jees.26.006

adsorption progressed, the rate gradually decreased due to the occupation of active sites and increasing diffusion resistance. Equilibrium was reached after approximately 180 min, beyond which no significant increase in adsorption capacity was observed. The rapid adsorption kinetics demonstrate the strong affinity between the pollutants and the functionalized rGO surface, highlighting the effectiveness of the material for wastewater treatment applications.

Figure 3C illustrates the influence of adsorbent dosage on pollutant removal efficiency. Increasing the dosage from 10 to 50 mg resulted in a substantial improvement in removal efficiency for all contaminants. This behavior is attributed to the increased number of adsorption sites and larger effective surface area available for pollutant uptake. Removal efficiencies increased from approximately 40% at the lowest dosage to over 90% at 50 mg. Further increases in dosage beyond 50 mg produced only marginal improvements, indicating that sufficient adsorption sites were already available to remove most of the pollutants from solution. This behavior is commonly observed in adsorption systems and may also be associated with partial aggregation of adsorbent particles at higher dosages, which can reduce the effective surface area. Therefore, 50 mg was selected as the optimum adsorbent dosage for subsequent studies.

The effect of initial pollutant concentration is shown in Figure 3D. The adsorption capacity increased steadily with increasing concentration from 10 to 200 mg/L for all pollutants. At low concentrations, the available adsorption sites greatly exceeded the number of pollutant molecules, resulting in relatively low adsorption capacities despite high removal efficiencies. As the concentration increased, a stronger concentration gradient developed between the bulk solution and the adsorbent surface, enhancing mass transfer and promoting greater adsorption uptake. The adsorption capacities gradually approached saturation at concentrations above 150 mg/L, reaching maximum values of approximately 110, 102, 95, and 108 mg/g for Cd^{2+}, Ni^{2+}, Pb^{2+}, and MB, respectively. Among the investigated contaminants, Cd^{2+} exhibited the highest adsorption capacity, followed closely by MB, while Pb^{2+} showed the lowest uptake. These differences are likely related to variations in ionic radius, hydration energy, and affinity toward the oxygen-containing functional groups present on the rGO surface.

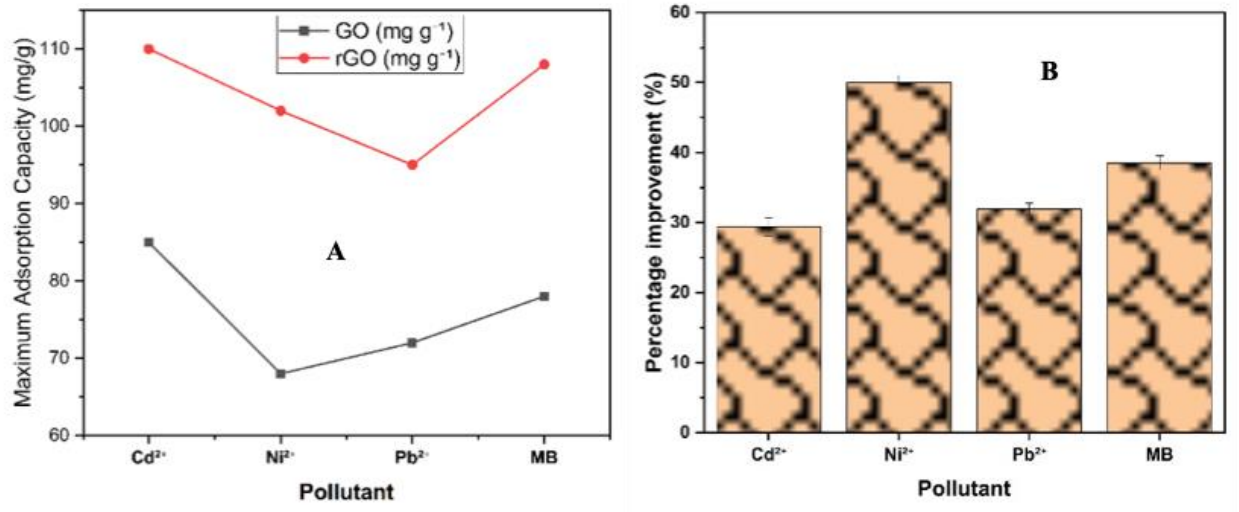

Figure 4. Comparison of the adsorption performance of GO-like nanosheets and rGO toward Cd^{2+}, Ni^{2+}, Pb^{2+}, and MB: (A) maximum adsorption capacities and (B) percentage improvement achieved after reduction of GO-like nanosheets to rGO.

https://doi.org/10.66973/jees.26.006

3.3 Comparative Adsorption Performance of GO-like Nanosheets and rGO

The adsorption performance of the synthesized GO-like nanosheets and rGO was compared using the maximum adsorption capacities obtained for Cd^{2+}, Ni^{2+}, Pb^{2+}, and MB, as shown in Figure 4A. A substantial enhancement in adsorption capacity was observed following the reduction process, demonstrating the positive impact of structural modification on the adsorption behaviour of the material. The adsorption capacities of the GO-like nanosheets were 85, 68, 72, and 78 mg/g for Cd^{2+}, Ni^{2+}, Pb^{2+}, and MB, respectively. Following chemical reduction, the adsorption capacities increased to 110, 102, 95, and 108 mg/g, respectively. Among the investigated pollutants, Cd^{2+} exhibited the highest adsorption capacity, followed closely by MB, whereas Pb^{2+} showed the lowest adsorption uptake. The superior performance toward Cd^{2+} may be attributed to its favourable ionic properties and stronger affinity toward oxygen-containing functional groups present on the rGO surface. In the case of MB, the high adsorption capacity is likely associated with strong π–π interactions between the aromatic dye molecules and the restored graphitic domains of rGO.

The percentage improvement resulting from the reduction process is presented in Figure 4B. The adsorption enhancement reached approximately 29.4% for Cd^{2+}, 50.0% for Ni^{2+}, 31.9% for Pb^{2+}, and 38.5% for MB. The most significant improvement was observed for Ni^{2+} adsorption, indicating that the reduction process substantially increased the accessibility and effectiveness of adsorption sites involved in metal ion binding. The enhancement observed for MB further confirms the beneficial role of restoring the sp^2 carbon network, which strengthens interactions between the graphene surface and aromatic organic molecules. The improved adsorption performance of rGO can be attributed to several structural changes occurring during reduction. Removal of oxygen-containing functional groups promotes partial restoration of graphitic domains, increases electronic conjugation, and improves surface accessibility. In addition, the reduction process generates a more porous and structurally ordered carbon framework, facilitating enhanced pollutant diffusion and adsorption. These changes collectively increase the number and effectiveness of active adsorption sites available for pollutant uptake.

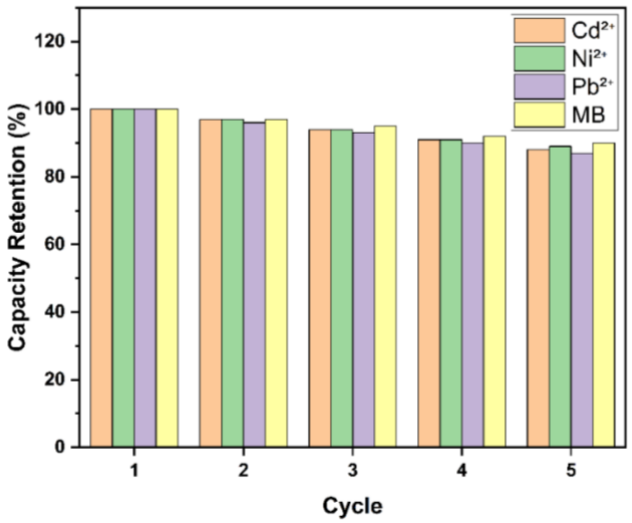

Figure 5. Regeneration and reusability performance of biomass-derived rGO for the adsorption of Cd^{2+}, Ni^{2+}, Pb^{2+}, and MB over five consecutive adsorption–desorption cycles.

https://doi.org/10.66973/jees.26.006

3.4 Regeneration and Reusability of rGO

The regeneration and reusability of an adsorbent are critical parameters for assessing its practical applicability in wastewater treatment. The stability of the synthesized biomass-derived rGO was evaluated through five consecutive adsorption–desorption cycles using Cd^{2+}, Ni^{2+}, Pb^{2+}, and MB as model pollutants. As shown in Figure 5, the adsorption capacity retention remained high throughout the regeneration experiments, demonstrating the excellent stability of the synthesized rGO. After the first adsorption cycle, all pollutants exhibited 100% capacity retention. Following five consecutive regeneration cycles, the adsorption capacities remained at approximately 88%, 89%, 87%, and 90% of their original values for Cd^{2+}, Ni^{2+}, Pb^{2+}, and MB, respectively. A gradual decrease in adsorption performance was observed with increasing cycle number, which is commonly attributed to incomplete desorption of pollutants, partial blockage of active adsorption sites, and minor structural changes occurring during repeated adsorption–desorption processes. Nevertheless, the observed reduction was relatively small, with capacity losses of only 10–13% after five cycles. Among the investigated pollutants, MB exhibited the highest retention efficiency, maintaining approximately 90% of its initial adsorption capacity after the fifth cycle, while Pb^{2+} showed the largest decrease, retaining approximately 87% of its original capacity. The excellent regeneration performance demonstrates the structural robustness of the rGO nanosheets and indicates that the adsorption process is largely reversible. The high retention efficiencies observed after repeated use suggest that the adsorbent maintains most of its active adsorption sites and surface functionality despite multiple regeneration treatments. This behaviour is consistent with the stable graphitic framework of rGO and its resistance to structural degradation during adsorption and desorption.

4 Conclusion

In this study, coconut shell waste was successfully valorized into biomass-derived reduced graphene oxide (rGO) through carbonization, modified Hummer's oxidation, and subsequent chemical reduction. The developed approach provides a sustainable and cost-effective route for converting agricultural waste into a value-added carbon nanomaterial for environmental remediation applications. Morphological characterization confirmed the successful transformation of the carbonized biomass into graphene oxide-like nanosheets and their subsequent reduction to rGO. SEM and TEM analyses revealed the formation of layered graphene-like structures and a more compact graphitic framework after reduction, indicating restoration of structural ordering and enhanced surface characteristics. The adsorption performance of the synthesized rGO was systematically evaluated toward Cd^{2+}, Ni^{2+}, Pb^{2+}, and methylene blue under different operating conditions. Adsorption was strongly influenced by solution pH, contact time, adsorbent dosage, and initial pollutant concentration. Optimal adsorption was achieved at approximately pH 7, with equilibrium reached after 180 min and an optimum adsorbent dosage of 50 mg. Under optimized conditions, the maximum adsorption capacities reached 110 mg/g for Cd^{2+}, 102 mg/g for Ni^{2+}, 95 mg/g for Pb^{2+}, and 108 mg/g for methylene blue, demonstrating the excellent affinity of rGO toward both heavy metals and organic dye pollutants. A direct comparison between the graphene oxide-like material and rGO revealed that chemical reduction substantially enhanced adsorption performance. The adsorption capacities increased by 29.4%, 50.0%, 31.9%, and 38.5% for Cd^{2+}, Ni^{2+}, Pb^{2+}, and methylene blue, respectively, highlighting the critical role of restoring graphitic domains and improving surface accessibility during the reduction process. The synthesized rGO also exhibited excellent regeneration capability and structural stability. After five consecutive adsorption–desorption cycles, the material retained approximately 88–90% of its original adsorption

https://doi.org/10.66973/jees.26.006

capacity, confirming its suitability for repeated use and practical wastewater treatment applications.

Authorship Contribution Statement

P.H., V.A., B.A.A.: Writing original draft, Methodology, Conceptualization. H.K.M.: Writing original draft, Methodology, Conceptualization, Supervision.

Conflict of Interest

Authors declare they have no known conflict of interest

Data availability

All required data will be available upon request from the corresponding authors.

REFERENCES:

[1] F. Fu and Q. Wang, "Removal of heavy metal ions from wastewaters: A review," *Journal of Environmental Management*, *92*(3), 407–418. https://doi.org/10.1016/j.jenvman.2010.11.011

[2] G. Crini and E. Lichtfouse, "Advantages and disadvantages of techniques used for wastewater treatment," *Environmental Chemistry Letters*, *17*(1), 145–155. https://doi.org/10.1007/s10311-018-0785-9

[3] D. Mohan and C. U. Pittman, "Arsenic removal from water/wastewater using adsorbents—A critical review," *Journal of Hazardous Materials*, *142*(1), 1–53. https://doi.org/10.1016/j.jhazmat.2007.01.006

[4] V. K. Gupta and Suhas, "Application of low-cost adsorbents for dye removal – A review," *Journal of Environmental Management*, *90*(8), 2313–2342. https://doi.org/10.1016/j.jenvman.2008.11.017

[5] S. Eberle, H. Börnick, and S. Stolte, "Granular Natural Zeolites: Cost-Effective Adsorbents for the Removal of Ammonium from Drinking Water," *Water*, *14*(6), 939. https://doi.org/10.3390/w14060939

[6] A. A. Basheer, "New generation nano-adsorbents for the removal of emerging contaminants in water," *Journal of Molecular Liquids*, *261*, 583–593. https://doi.org/10.1016/j.molliq.2018.04.021

[7] A. Bhatnagar and M. Sillanpää, "Utilization of agro-industrial and municipal waste materials as potential adsorbents for water treatment—A review," *Chemical Engineering Journal*, *157*(2), 277–296. https://doi.org/10.1016/j.cej.2010.01.007

[8] A. Ibrahim, M. S. Vohra, S. A. Bahadi, S. A. Onaizi, M. H. Essa, and T. Mohammed, "Heavy metals adsorption onto graphene oxide: effect of mixed systems and response surface methodology modeling," *Desalination and Water Treatment*, *266*, 78–90. https://doi.org/10.5004/dwt.2022.28615

[9] F. Liu, S. Chung, G. Oh, and T. S. Seo, "Three-Dimensional Graphene Oxide Nanostructure for Fast and Efficient Water-Soluble Dye Removal," *ACS Applied Materials & Interfaces*, *4*(2), 922–927. https://doi.org/10.1021/am201590z

[10] P. Gabdullin, A. Zhurkin, V. Osipov, N. Besedina, O. Kvashenkina, and A. Arkhipov, "Thin carbon films: Correlation between morphology and field-emission capability," *Diamond and Related Materials*, *105*, 107805. https://doi.org/10.1016/j.diamond.2020.107805

[11] A. K. Geim and K. S. Novoselov, "The rise of graphene," *Nature Materials*, *6*(3), 183–191. https://doi.org/10.1038/nmat1849

[12] D. R. Dreyer, S. Park, C. W. Bielawski, and R. S. Ruoff, "The chemistry of graphene oxide," *Chemical Society Reviews*, *39*(1), 228–240. https://doi.org/10.1039/B917103G

[13] S.-T. Yang, S. Chen, Y. Chang, A. Cao, Y. Liu, and H. Wang, "Removal of methylene blue from aqueous solution by graphene oxide," *Journal of Colloid and Interface Science*, *359*(1), 24–29. https://doi.org/10.1016/j.jcis.2011.02.064

[14] L. Liu *et al.*, "Graphene-based polymer composites in thermal management: materials, structures and applications," *Materials Horizons*, *12*(1), 64–91. https://doi.org/10.1039/D4MH00846D

https://doi.org/10.66973/jees.26.006

[15] A. T. Smith, A. M. LaChance, S. Zeng, B. Liu, and L. Sun, "Synthesis, properties, and applications of graphene oxide/reduced graphene oxide and their nanocomposites," *Nano Materials Science*, *1*(1), 31–47. https://doi.org/10.1016/j.nanoms.2019.02.004

[16] K. Cao, Z. Tian, X. Zhang, Y. Wang, and Q. Zhu, "Green preparation of graphene oxide nanosheets as adsorbent," *Scientific Reports*, *13*(1), 9314. https://doi.org/10.1038/s41598-023-36595-2

[17] D. C. Marcano *et al.*, "Improved Synthesis of Graphene Oxide," *ACS Nano*, *4*(8), 4806–4814. https://doi.org/10.1021/nn1006368

[18] O. M. El-Borady, "Wastewater Treatment using Innovative Green-Synthesized rGO, TiO2NPs, and rGO/TiO2 Nanocomposite: Structural, Morphological, Spectroscopic, Thermal, and Photocatalytic Studies," *Water, Air, & Soil Pollution*, *236*(2), 75. https://doi.org/10.1007/s11270-024-07692-3

[19] M. Blachnio, A. Derylo-Marczewska, B. Charmas, M. Zienkiewicz-Strzalka, V. Bogatyrov, and M. Galaburda, "Activated Carbon from Agricultural Wastes for Adsorption of Organic Pollutants," *Molecules*, *25*(21), 5105. https://doi.org/10.3390/molecules25215105

[20] E. H. Sujiono *et al.*, "Graphene oxide based coconut shell waste: synthesis by modified Hummers method and characterization," *Heliyon*, *6*(8), e04568. https://doi.org/10.1016/j.heliyon.2020.e04568

[21] D. Castro, N. Ma. Rosas-Laverde, M. B. Aldás, C. E. Almeida-Naranjo, V. H. Guerrero, and A. I. Pruna, "Chemical Modification of Agro-Industrial Waste-Based Bioadsorbents for Enhanced Removal of Zn(II) Ions from Aqueous Solutions," *Materials*, *14*(9), 2134. https://doi.org/10.3390/ma14092134

[22] A. Nishat *et al.*, "Wastewater treatment: A short assessment on available techniques," *Alexandria Engineering Journal*, *76*, 505–516. https://doi.org/10.1016/j.aej.2023.06.054